Hyperaccurate thermoelectric currents

André M. Timpanaro,[1] Giacomo Guarnieri,[2] and Gabriel T. Landi[3]
[1]*Centro de Matemática, Computação e Cognição, Universidade Federal do ABC, 09210-580 Santo André, Brazil*
[2]*Dahlem Center for Complex Quantum Systems, Freie Universität Berlin, 14195 Berlin, Germany*
[3]*Instituto de Física da Universidade de São Paulo, 05314-970 São Paulo, Brazil*

(Received 13 September 2021; revised 27 September 2022; accepted 23 February 2023; published 31 March 2023)

Thermodynamic currents, such as energy, heat, and entropy production, can fluctuate significantly at the nanoscale. However, some fluctuate less than others. Hyperaccurate currents are defined as those which fluctuate the least, in the sense that they maximize the signal-to-noise ratio (precision). In this Letter we analytically determine what are the hyperaccurate currents in quantum thermoelectrics, modeled by coherent transport in the Landauer-Büttiker formalism. Our results yield a tight and general bound on precision, which replace the classical thermodynamic uncertainty relations, that can be violated in quantum thermoelectrics. They also allow us to address the question of how close to hyperaccurate is a given current. We illustrate our findings for smooth boxcar functions, and for a double quantum dot operating as a thermal machine. In the latter, we use our results to establish the parameter ranges for which the output power of an autonomous engine can become hyperaccurate arbitrarily far from equilibrium.

DOI: 10.1103/PhysRevB.107.115432

I. INTRODUCTION

Fluctuations of the power grid can potentially fry our electronics, a fact which is widely taken into account in chip manufacturing. Such fluctuations become even more relevant at the nanoscale, the endpoint of the miniaturization march. Consequently, strategies for curbing them demand increasing attention. For thermodynamic currents, such as energy, charge, heat, or work, the precision is determined by their signal-to-noise ratio (SNR)

$$\mathcal{S}_J = J^2/\Delta_J^2, \tag{1}$$

where J denotes the average current and Δ_J^2 its corresponding variance. Different currents can clearly be more or less sensitive to fluctuations. For instance, in a thermoelectric engine the fluctuations of the output power can behave very differently from that of the heat fluxes. In recent years there has been a boom of interest in determining, and achieving, upper bounds for any SNR, as they allow one to quantify its ultimate reliability.

A central result in this context was provided by the so-called Thermodynamic Uncertainty Relations (TURs) [1–4], which, in classical Markov processes, bounds the SNR in terms of the average entropy production rate σ, according to

$$\mathcal{S}_J \leqslant \sigma/2. \tag{2}$$

This result implies that to improve precision, one must pay a price in dissipation [5–9]. The bound (2) can generally be quite loose, however, even for classical machines. To quantitatively address this fact, Busiello and Pigolotti recently introduced the concept of a *hyperaccurate current* [10] as the one which possesses the maximum SNR $\mathcal{S}_{\rm hyp}$ among all currents, i.e.,

$$\mathcal{S}_J \leqslant \mathcal{S}_{\rm hyp}. \tag{3}$$

Taken together, Eqs. (2) and (3) imply the following sequence of bounds $\mathcal{S}_J \leqslant \mathcal{S}_{\rm hyp} \leqslant \sigma/2$. Unlike the TUR, however, the bound (3) is always *saturable*. This is therefore of value even if the hyperaccurate current itself is not easily accessible, for it allows one to determine how close a given physical current is from being hyperaccurate. For instance, the entropy production rate only becomes hyperaccurate (i.e., $\mathcal{S}_\sigma \equiv \mathcal{S}_{\rm hyp}$) when the Fluctuation Dissipation Relation (FDR), $\Delta_\sigma^2 = 2\sigma$, is satisfied, which also implies that $\mathcal{S}_\sigma = \sigma/2$, i.e., TUR is saturated [11].

In the presence of quantum effects, however, coherent transport, as opposed to incoherent transitions, make violations of Eq. (2) possible [12–22]; i.e., $\mathcal{S}_J \nleqslant \sigma/2$. This means one can improve precision without necessarily increasing the dissipation. One is therefore naturally led to ask whether a quantum version of the hyperaccurate current can be found. By definition, this would then replace the TUR and, at the same time, provide a fundamental and saturable upper bound on the SNR of any current, i.e., $\mathcal{S}_\sigma \equiv \mathcal{S}_{\rm hyp}$. It can also help to shed light on the mechanisms which make a certain current more or less accurate. In this Letter we answer this question for quantum thermoelectric systems undergoing coherent transport, as described by the Landauer-Büttiker formalism. In particular, we prove two main results. First, we obtain a closed formula for the hyperaccurate current in the Landauer-Büttiker context, which is straightforward to evaluate and provides the ultimate cap on precision. However, as we show, this current is a nonlinear functional of energy and therefore the bound is never strictly saturated by a thermodynamic current, such as heat and output power. To address this, we derive a second upper bound, called thermal-hyperaccurate, $\mathcal{S}_{\rm thyp}$, which optimizes only over the subset of thermodynamic currents. To illustrate the significance of our findings, we study smoothed boxcar transmission functions, and a double quantum dot operating as a thermal machine.

TABLE I. List of physical currents: [Eq. (4)] and their corresponding variances [Eq. (5)]. The SNR is $\mathcal{S}_h = J_h^2/\Delta_h^2$. Here P is the output power, J_{Q_i} are the heat currents ($i = L, R$), and σ is the entropy production. Power and heat are defined so that $P + J_Q^L + J_Q^R = 0$. The last two lines refer to the hyperaccurate and linear-hyperaccurate bounds in Theorems 1 and 2. All δ's are "left minus right:" $\delta_\beta = \beta_L - \beta_R$, $\delta_\mu = \mu_L - \mu_R$ and $\delta_{\beta\mu} = \beta_L\mu_L - \beta_R\mu_R$. Finally, C_{ij} is the covariance between two currents, defined in Eq. (6).

Current	$h(\epsilon)$	Variance
J_N	1	Δ_N^2
J_E	ϵ	Δ_E^2
$P = -\delta_\mu J_N$	$-\delta_\mu$	$\Delta_P^2 = \delta_\mu^2 \Delta_N^2$
$J_{Q_R} = J_E - \mu_R J_N$	$\epsilon - \mu_R$	$\Delta_{Q_R}^2 = \Delta_E^2 - 2\mu_R C_{NE} + \mu_R^2 \Delta_N^2$
$J_Q^L = \mu_L J_N - J_E$	$\mu_L - \epsilon$	$\Delta_{Q_L}^2 = \Delta_E^2 - 2\mu_L C_{NE} + \mu_L^2 \Delta_N^2$
$\sigma = -\delta_\beta J_E + \delta_{\beta\mu} J_N$	$-\delta_\beta \epsilon + \delta_{\beta\mu}$	$\Delta_\sigma^2 = \delta_\beta^2 \Delta_E^2 + \delta_{\beta\mu}^2 \Delta_N^2 - 2\delta_\beta \delta_{\beta\mu} C_{NE}$
J_{hyp}	Eq. (8)	Eq. (9)
$J_{\text{thyp}} = aJ_{Q_R} + bJ_N$	Eq. (10)	Eq. (11)

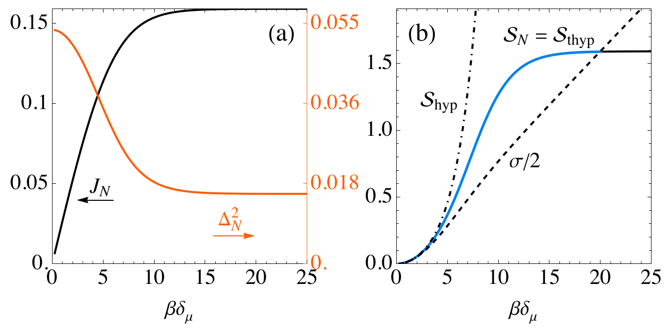

FIG. 1. (a) Average particle current J_N, and particle current fluctuations Δ_N^2, for the smooth boxcar (7), as a function of the chemical potential bias $\beta\delta_\mu$, with constant $\beta_L = \beta_R = \beta$. (b) Signal-to-noise ratio $\mathcal{S}_N = J_N^2/\Delta_N^2$. The region for which the curve is blue represents violations of the classical TUR (2). Also shown is our new hyperaccurate bound, $\mathcal{S}_{\text{hyp}}$ [Eq. (9)]. In this case $\mathcal{S}_N = \mathcal{S}_{\text{thyp}}$, so that the particle current is the thermal hyperaccurate current. Parameters: $\beta a = 2.5$, $\beta\gamma = 0.5$.

II. LANDAUER-BüTTIKER FORMALISM

We consider a quantum thermoelectric system characterized by an energy-dependent transmission function $\mathcal{T}(\epsilon) \in [0, 1]$. The system is coupled to two baths $i = L, R$, kept at different inverse temperatures $\beta_i = 1/T_i$ (we set $k_B = 1$), and chemical potentials $\mu_i = eV_i$, where e is the electric charge and V_i the voltage difference. A generic current, within the Landauer-Büttiker formalism, has the form (we set $\hbar = 1$) [23,24]

$$J_h = \int d\epsilon\ h(\epsilon)\mathcal{T}(\epsilon)\delta f(\epsilon), \tag{4}$$

where $\delta f = f_L - f_R$ and $f_i(\epsilon) = (e^{\beta_i(\epsilon-\mu_i)} + 1)^{-1}$ is the Fermi-Dirac occupation of bath i. Here $h(\epsilon)$ defines the type of current in question: the particle current J_N corresponds to $h(\epsilon) = 1$, and the energy current J_E to $h(\epsilon) = \epsilon$. Other currents, such as heat, output power and entropy production, are defined similarly, and summarized in Table I. More complicated functions $h(\epsilon)$, despite not being typical, are also physically allowed (as proven in Appendix C). Within the Levitov-Lesovik full-counting formalism [25,26], the variance associated to any such current reads

$$\Delta_h^2 = \int d\epsilon\ h^2\mathcal{T}[g + \delta f^2(1 - \mathcal{T})], \tag{5}$$

where $g = f_L(1 - f_L) + f_R(1 - f_R)$ and the argument ϵ of the functions was omitted for clarity. The SNR (1) is then $\mathcal{S}_h = J_h^2/\Delta_h^2$. We also introduce the covariance C_{ij} between currents $h_i(\epsilon)$ and $h_j(\epsilon)$ [16]:

$$C_{ij} = \int d\epsilon\ h_i h_j \mathcal{T}[g + \delta f^2(1 - \mathcal{T})]. \tag{6}$$

Equivalent formulas can also be obtained using current-current correlators [27].

Before we introduce our main results, let us motivate them through an example. Consider a thermoelectric device under a voltage bias δ_μ and no temperature bias ($T_L = T_R$). The transmission function is taken to be a smooth boxcar [18,28,29]:

$$\mathcal{T}(\epsilon) = \frac{1}{2}\left[\tanh\frac{\epsilon + a}{\gamma} - \tanh\frac{\epsilon - a}{\gamma}\right], \tag{7}$$

where γ is the smoothness factor, and $2a$ is the width. Boxcars have long been studied in the context of thermal machines [29]. Recently, it was also shown that they lead to TUR violations, which are only recovered in the large voltage bias limit [30]. Figure 1(a) shows the average particle current J_N, and its variance Δ_N^2, as a function of the chemical potential bias $\beta\delta_\mu$. Since $\beta_L = \beta_R$, the entropy production rate is simply $\sigma = \beta\delta_\mu J_N$. Upon increasing the drive $\beta\delta_\mu$, the current grows while the fluctuations diminish. The corresponding SNR $\mathcal{S}_N$ [Fig. 1(b)] therefore grows as well. For this model, the classical TUR (2), no longer places a bound on the maximum precision achievable by the particle current, as shown in Fig. 1(b).

Therefore, this highlights at least two important questions: (i) In the absence of the TUR, what ultimately bounds the precision? (ii) Are there other currents which can be more precise than J_N? Our main results, summarized in Theorems 1 and 2 below, provide definitive answers to these questions. Theorem 1 establishes the fundamental hyperaccurate bound $\mathcal{S}_{\text{hyp}}$ [dot dashed line in Fig. 1(b)] while Theorem 2 establishes the best possible precision, $\mathcal{S}_{\text{thyp}}$ ("thermal hyperaccurate"), achievable by actual thermodynamic currents, i.e., heats and output power. In the example of Fig. 1(b), it turns out that the particle current itself (and the entropy production) are thermalhyperaccurate.

III. MAIN RESULTS

Theorem 1 ("hyp"): For given transmission function $\mathcal{T}(\epsilon)$ and parameters (T_L, T_R, μ_L, μ_R), the current which maximizes the SNR (1) is the one corresponding to

$$h_{\text{hyp}}(\epsilon) \propto \frac{\delta f(\epsilon)}{g(\epsilon) + \delta f(\epsilon)^2[1 - \mathcal{T}(\epsilon)]}. \tag{8}$$

The related optimal SNR is given by

$$\mathcal{S}_{\rm hyp} = \int d\epsilon \frac{\delta f(\epsilon)^2 \mathcal{T}(\epsilon)}{g(\epsilon) + \delta f(\epsilon)^2(1-\mathcal{T}(\epsilon))}. \tag{9}$$

Since the SNR is invariant to a change $h \to \alpha h$, Eq. (8) is only defined up to a scale.

Proof: Since the problem is invariant under a change of scale, to maximize J_h^2/Δ_h^2 we can, without loss of generality, also fix the scale so that $J_h \equiv 1$. The problem then becomes that of minimizing Δ_h^2 over $h(\epsilon)$, subject to the constraint that $J_h = 1$. This is a convex optimization problem and can thus be treated with standard Lagrange multipliers. We introduce the functional $G[h(\epsilon)] = \Delta_h^2/J_h^2 + \lambda(J_h - 1)$, where λ is a Lagrange multiplier. Minimizing over $h(\epsilon)$, through standard variational calculus, yields Eq. (8). Finally, substituting $h_{\rm hyp}$ in Eqs. (4) and (5), leads to (9). ■

The bound (9) is straightforward to compute, requiring only a single integral. It also simplifies considerably whenever $\mathcal{T}$ is sharply windowed between zero or one, which encompasses the important examples of boxcars [18,28–30] and quantum point contacts [31,32]. The scale invariance of Eq. (8) can be made to match the choice of Ref. [10], for which $\Delta^2_{\rm hyp} = 2J_{\rm hyp}$ such that $\mathcal{S}_{\rm hyp} = J_{\rm hyp}/2$. The hyperaccurate current is also gauge invariant, like J_N, J_{Q_i}, and P [33].

However, the fact that the $h_{\rm hyp}$ is a complicated function of ϵ means it is generally not accessible in the laboratory. Hence, even though Eq. (9) provides a universal bound, it will generally not be saturated by thermodynamic currents, which are always of the form $h(\epsilon) = a\epsilon + b$. To address this, we next consider an optimization only over currents of this form. In order to make it explicitly gauge invariant, we parametrize without loss of generality $h(\epsilon) = a(\epsilon - \mu_R) + b$. We refer to these as "thermal hyperaccurate." This leads to our second main result:

Theorem 2 ("thyp"): Restricting to currents of the form $h(\epsilon) = a(\epsilon - \mu_R) + b$, the hyperaccurate current is the one that satisfies

$$\frac{b}{a} = \frac{J_N \Delta^2_{Q_R} - J_{Q_R} C_{Q_R,N}}{J_{Q_R}\Delta_N^2 - J_N C_{Q_R,N}}. \tag{10}$$

The corresponding optimal SNR reads

$$\mathcal{S}_{\rm thyp} = \frac{J_N^2 \Delta^2_{Q_R} + J^2_{Q_R}\Delta_N^2 - 2J_N J_{Q_R} C_{Q_R,N}}{\Delta^2_{Q_R}\Delta^2_N - C^2_{Q_R,N}}. \tag{11}$$

Combined with Theorem 1, it thus follows that for any thermodynamic current

$$\mathcal{S}_J \leqslant \mathcal{S}_{\rm thyp} \leqslant \mathcal{S}_{\rm hyp}. \tag{12}$$

Proof: Due to scale invariance, to maximize the SNR we can minimize Δ_h^2 over a and b, with fixed $J_h = J_0$, which can be with standard Lagrange multipliers. ■

If $T_L = T_R$, $\mu_L = -\mu_R$, and $\mathcal{T}(\epsilon)\delta f(\epsilon)$ is an even function of ϵ, one may verify that J_N becomes thermalhyperaccurate [Fig. 1(b)]. Conversely, if $\mu_L = \mu_R = 0$ and $\mathcal{T}\delta f$ is an odd function of ϵ, then $J_{Q_L} \equiv J_{Q_R}$ become thermalhyperaccurate instead. In other cases, the thermal-hyperaccurate current will usually be a nontrivial mixture of heat and particle currents.

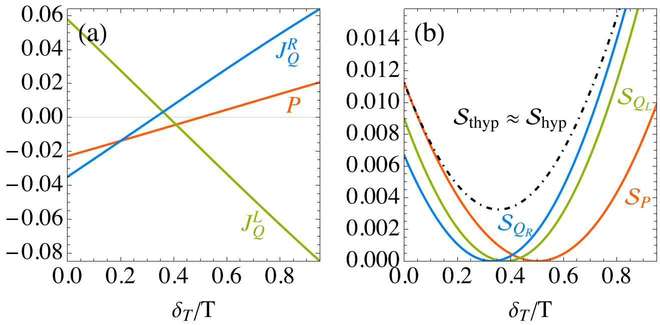

FIG. 2. Thermodynamic properties of a double quantum dot engine [Eq. (13)] as a function of the temperature gradient $\delta_T/T = (T_L - T_R)/T$, with fixed $T = (T_L + T_R)/2$. (a) Average heat currents $J_Q^{L(R)}$, and average output power P. The system operates as an engine when $P, J_Q^L, J_Q^R > 0$. (b) Corresponding SNRs. The black dot dashed curve is the linear hyperaccurate bound (11). For low δ_T the output power is nearly hyperaccurate. But for high δ_T, the situation reverses. Parameters: $\beta\Gamma = \beta\Omega = \beta\epsilon/2 = 1$, $\beta\mu_R = -\beta\mu_L = 0.35$.

IV. DOUBLE QUANTUM DOT THERMAL MACHINE

We illustrate our results by studying a double quantum dot, defined by the transmission function [13]

$$\mathcal{T}(\epsilon) = \frac{\Gamma^2\Omega^2}{|(\epsilon - \epsilon_0 + i\Gamma/2)^2 - \Omega^2|^2}, \tag{13}$$

where Γ is the bath coupling strength (in the wide-band limit), ϵ_0 the dot energy, and Ω the inter-dot coupling. In Fig. 2(a) we plot the average output power P, and the average heat currents $J_{Q_{L(R)}}$ to the two baths (cf. Table I for definitions), as a function of $\delta_T/T = (T_L - T_R)/T$. The system operates as an autonomous engine when $P, J_{Q_R} > 0$ and $J_{Q_L} < 0$ [34].

The corresponding SNRs of the three quantities are shown in Fig. 2(b), with $\mathcal{S}_{\rm thyp}$ shown as dot dashed. In this particular case, $\mathcal{S}_{thyp} \simeq \mathcal{S}_{\rm hyp}$. We can thus use our results to address the accuracy of each current. For low thermal gradients the output power is found to be nearly hyperaccurate. This happens because low δ_T yields heat currents which are small on average, but whose fluctuations are nonnegligible, causing the signal-to-noise ratio $\mathcal{S}_{Q_i}$ to fall significantly. For large δ_T the situation reverses, and the current to the cold bath J_{Q_R} becomes nearly hyperaccurate. We therefore see that the precision characteristics are very different in the domain where the dots operate as an engine or not.

We can analyze how close the output power is to being thermalhyperaccurate. In Fig. 3(a) we plot $\mathcal{S}_P/\mathcal{S}_{\rm thyp}$ as a function of $\delta\mu/T = (\mu_L - \mu_R)/T$ for different values of $\delta_T/T = (T_L - T_R)/T$, where $T = (T_L + T_R)/2$. As is clear from the image, the output power becomes hyperaccurate for sufficiently large δ_μ. For moderate δ_μ, the precision of P will depend on δ_T [in agreement with Fig. 2(b)]. A similar analysis is shown in Fig. 3(b) for the entropy production σ. It is found that for most parameter ranges, σ is close to thermal hyperaccurate. The discrepancy, however, is more significant for large δ_T.

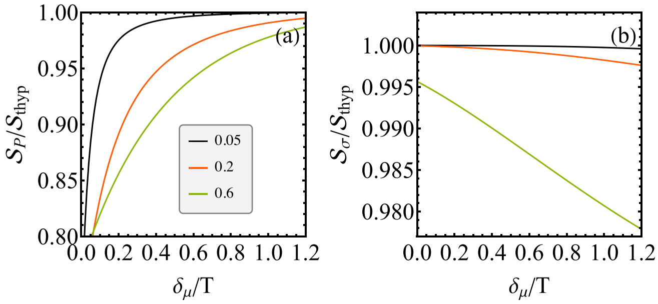

FIG. 3. How accurate is the output power and entropy production? The curves represent the ratio (a) $\mathcal{S}_P/\mathcal{S}_{\rm thyp}$ and (b) $\mathcal{S}_{Q_R}/\mathcal{S}_{\rm thyp}$, with respect to the thermal hyperaccurate bound (11), as a function of $\delta\mu/T = (\mu_L - \mu_R)/T$. Each curve is for a different value of $\delta_T/T = (T_L - T_R)/T$, where $T = (T_L + T_R)/2$. From top to bottom: $\delta_T/T = 0.05, 0.2, 0.6$.

V. SMALL BIASES REGIME

The previous example indicates that for small biases (linear response regime), the entropy production becomes thermal-hyperaccurate. To understand this in more general terms, we carry out a systematic expansion of our two bounds in terms of the biases δ_β and $\delta_{\beta\mu}$. We parametrize

$$\beta_{L(R)} = \beta \pm \delta_\beta/2, \quad \beta_{L(R)}\mu_{L(R)} = \beta\mu \pm \delta_{\beta\mu}/2. \tag{14}$$

Expanding in terms of $\delta_{\beta\mu}$ is mathematically more convenient. To convert to δ_μ simply use $\delta_{\beta\mu} = \beta\delta_\mu + \mu\delta_\beta + \delta_\beta\delta_\mu$. A fourth order series expansion of all currents considered in this Letter, as well as their fluctuations, is reported in Appendix D. Here we focus specifically on Theorems 1 and 2. The entropy production, up to fourth order in the biases, reads

$$\sigma = \sigma^{(2)} + \Theta_4/24. \tag{15}$$

Here $\sigma^{(2)} = \delta_\beta^2\theta_2 - 2\delta_\beta\delta_{\beta\mu}\theta_1 + \delta_{\beta\mu}^2\theta_0$ is the lowest order contribution, with $\theta_n = \int d\epsilon\epsilon^n f(1-f)\mathcal{T}$ and $f = (e^{\beta(\epsilon-\mu)} + 1)^{-1}$ being the Fermi function evaluated at the average temperature and chemical potential. The last term in Eq. (15), on the other hand, reads $\Theta_4 = \int d\epsilon(\delta_{\beta\mu} - \epsilon\delta_\beta)^4 f(1-f)(1-6f+6f^2)\mathcal{T}$, which is a fourth-order contribution in δ_β and $\delta_{\beta\mu}$.

We compute similar expansions for both $\mathcal{S}_{\rm hyp}$ [Eq. (9)] and $\mathcal{S}_{\rm thyp}$ [Eq. (11)]. It is found that they coincide to the fourth order, and are given by

$$\mathcal{S}_{\rm hyp} = \mathcal{S}_{\rm thyp} = \frac{\sigma}{2} - (\Theta_4 + 6\Psi_4)/24, \tag{16}$$

where $\Psi_4 = \int d\epsilon(\delta_{\beta\mu} - \epsilon\delta_\beta)^4 f^2(1-f)^2\mathcal{T}(1-\mathcal{T})$ is also a fourth-order contribution.

We thus reach the following conclusions. Both bounds coincide to the fourth order. And they coincide with the classical TUR (2) only up to the second order. The entropy production thus becomes hyperaccurate, but only to the lowest order (where it also satisfies the FDR $\Delta_\sigma^2 = 2\sigma$). This is in agreement with Fig. 3. Deviations from the TUR appear at the fourth order. If $\mathcal{S}_{\rm (t)hyp} < \sigma/2$, the TUR will hold, but will never be saturated. And if $\mathcal{S}_{\rm (t)hyp} > \sigma/2$, then there definitely exists a thermodynamic current (the hyperaccurate one) which violates the TUR.

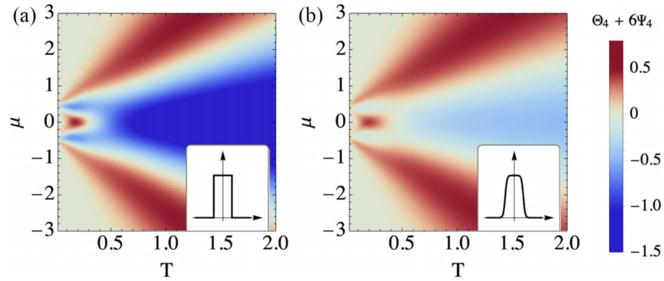

FIG. 4. Factor $(\Theta_4 + 6\Psi_4)/\delta_\beta^4$ (assuming $\delta_{\beta\mu} = 0$) in Eq. (16), as a function of T and μ, for the boxcar transmission function (7). Negative (blue) means the classical TUR can be violated. (a) Sharp boxcar, $a = 1/2$, $\gamma = 0$. (b) Smoothed boxcar, $a = 1/2$, $\gamma = 0.1$.

Using our results, we can provide guidelines on how $\mathcal{T}$ must behave in order to obtain TUR violations. The term Ψ_4 is always nonnegative, and therefore contributes toward making $\mathcal{S}_{\rm (t)hyp} < \sigma/2$. The first strategy is thus to suppress Ψ_4. Since it depends on $\mathcal{T}(1-\mathcal{T})$, it is minimized by transmission functions that are sharply windowed, changing quickly from zero to one. This is in agreement with Refs. [22,30,35], where TUR violations were found to be largest for boxcar functions. The term Θ_4, on the other hand, can have any sign. The function $f(1-f)(1-6f+6f^2)$ has a negative minimum around $\epsilon = \mu$, and remains negative only over a window of width of $\sim 2T$. Large TUR violations are thus precise when the transmission function is a boxcar centered around μ, and of width $\sim 2T$. Figure 4 illustrates the idea,where we plot the factor $\Theta_4 + 6\Psi_4$ for the boxcar transmission function defined in Eq. (7). Negative (blue) regions mean that there definitely exists a current which will violate the classical TUR.

VI. CONCLUSIONS

Thermodynamic uncertainty relations have become one of the central results to characterize current fluctuations arbitrarily far from equilibrium. However, the standard TUR is not valid in the quantum regime, leading to the question of whether a new universal upper bound on the signal-to-noise ratio of currents exist. In this Letter we provide a definitive answer to this question in terms of the current which possess the highest possible SNR for any given set of biases and transmission function, called the hyperaccurate current. Our bounds are valid for processes arbitrarily far from equilibrium, and are easily computable. Moreover, they can always be saturated by physically motivated processes, allowing one to unambiguously establish how hyperaccurate is a given thermodynamic current.

We also showed how our new bounds can be used to determine the precise parameter range for the temperature and voltage biases for which, given a certain transmission function, a desired target current can become hyperaccurate. While our results focused on the steady of a two terminal setup, they can be readily extended to multiterminal devices and time-dependent drives. Similarly, one can also in principle extend it to include bulk noises, in the form of Büttiker probes.

ACKNOWLEDGMENTS

The authors acknowledge fruitful discussions with R. Andrade, A. M. Cunha, A. Teixeira, I. Ferreira, I. Queiroz, M. Grael, K. Kunze, L. Busá, M. Jacobs, and G. Tamberi. G.T.L. acknowledges the financial support of the São Paulo Funding Agency FAPESP (Grants No. 2017/50304-7, No. 2017/07973-5, and No. 2018/12813-0), the Gridanian Research Council (GRC), and the Brazilian funding agency CNPq (Grant No. INCT-IQ 246569/2014-0). G.G. acknowledges support from FQXi and DFG FOR2724 and also from the European Union Horizon 2020 research and innovation program under the Marie Sklodowska-Curie Grant No. 101026667.

APPENDIX A: BASIC NOTATION AND THE TWO-POINT MEASUREMENT SCHEME

We consider a quantum system with initial state $\hat{\rho}$, evolving unitarily with evolution operator $\hat{U}(t, t_0)$. Let $\hat{O}(t) = \sum_{o_t} o_t \hat{\Pi}_{o_t}$ denote a generic observable, with eigenvalues o_t and projectors $\hat{\Pi}_{o_t}$. Throughout, we will repeatedly make use of the spectral theorem, which states that given an operator $\hat{O}$, as above, a generic function of it will have the following decomposition

$$f(\hat{O}_t) = \sum_{o_t} f(o_t)\hat{\Pi}_{o_t}. \tag{A1}$$

Within the two-point measurement (TPM) scheme, the probability of observing o_{t_i} at time t_i and then o_t at time t is given by

$$p_t(\Delta o) = \sum_{o_i, o_t} \delta(\Delta o - (o_t - o_i)) \times \mathrm{Tr}[\hat{\Pi}_{o_t}\hat{U}(t, t_i)\hat{\Pi}_{o_i}\hat{\rho}(t_i)\hat{\Pi}_{o_i}\hat{U}^\dagger(t, t_i)\hat{\Pi}_{o_t}], \tag{A2}$$

with $\delta(.)$ denoting the Dirac's delta function and $\hat{\rho}(t_i)$ being the initial state. We also define the cumulant generating function (CGF)

$$\mathcal{G}(\eta)_t = \ln \int d(\Delta o) e^{-i\eta\Delta o} p_t(\Delta o). \tag{A3}$$

From this, the variance can be obtained by differentiating over η: $\langle(\Delta o_t)^2\rangle = (-i)^2\partial_{\eta^2}\mathcal{G}(\eta)_t|_{\eta=0}$. Assuming that the initial density matrix $\hat{\rho}(t_i)$ commutes with $\hat{O}_{t_i}$, it is also possible to to rewrite the CGF as

$$\mathcal{G}_t(\eta) = \ln \mathrm{Tr}[e^{i\eta\hat{O}_t}\hat{U}(t, t_i)e^{i\eta\hat{O}_i}\hat{\rho}(t_i)\hat{U}^\dagger(t, t_i)]. \tag{A4}$$

APPENDIX B: FULL COUNTING STATISTICS FOR HYPERACCURATE FERMIONIC CURRENT IN QUANTUM THERMOELECTRIC SYSTEMS

We now analyze the CGF in the case of noninteracting fermions. We consider a composite system, with total Hamiltonian

$$\hat{\mathcal{H}} = \hat{\mathcal{H}}_S + \sum_\alpha (\hat{\mathcal{H}}_\alpha + \hat{V}_{S\alpha}), \ (\alpha = L, R). \tag{B1}$$

The first term is the Hamiltonian of the system, which is taken to be described by a quadratic Hamiltonian in a set of fermionic operators c_s; that is, $\hat{\mathcal{H}}_S = \sum_s \epsilon_s \hat{c}_s^\dagger \hat{c}_s$. This system functions as a junction, connecting a left and right bath, with Hamiltonians $\hat{\mathcal{H}}_{L(R)} = \sum_{l(r)} \epsilon_{l(r)} \hat{c}_{l(r)}^\dagger \hat{c}_{l(r)}$. Finally $\hat{V}_{SL(R)} = \sum_{s,l(r)}(J_{sl(r)}\hat{c}_s^\dagger \hat{c}_{l(r)} + \mathrm{H.c.})$ is the corresponding interaction. The above creation and annihilation operators for the system and the leads are fermionic operators each satisfying their own standard anticommutation relations $\{\hat{c}_j, \hat{c}_k^\dagger\} = \delta_{jk}$, $\hat{c}_j\hat{c}_k = \hat{c}_j^\dagger\hat{c}_k^\dagger = 0$.

Usually, the observable that is considered is either the particle number $\hat{N}_L$ or the energy $\hat{\mathcal{H}}_L$ of one of the reservoirs, say the left one for concreteness.

But here we will be interested in measuring a generic observable of the form $\hat{O}_h = h(\hat{\mathcal{H}}_L)$. By virtue of the spectral theorem Eq. (A1), its spectral decomposition in the Fock basis is given by

$$\hat{O}_h = h(\hat{\mathcal{H}}_L) = \sum_l h(\epsilon_l)\hat{c}_l^\dagger\hat{c}_l. \tag{B2}$$

Thus, by construction, this observable does not have coherences between different Fock states, and commutes with both the Hamiltonian and the particle number operator of the left reservoir. In order to be able to apply the TPM formalism of the previous section, one finally needs to consider an initial state which commutes with the desired observable, $\hat{O}_h$. We take, as is standard, the assumption that the interactions $\hat{V}_{SL} + \hat{V}_{SR}$ are adiabatically switched on from $t_i = -\infty$, so that the initial state has the form $\hat{\rho}(-\infty) = \hat{\rho}_S(-\infty)\bigotimes_{\alpha=L,R} Z_\alpha^{-1}\exp[-\beta_\alpha(\hat{\mathcal{H}}_\alpha - \mu_\alpha\hat{N}_\alpha)]$. We remark that the choice of the initial state for the central junction system is immaterial in the steady-state after the thermodynamic limit is performed in the baths [36]. We will therefore choose $\hat{\rho}_S(-\infty) = Z_S^{-1}e^{-\beta_S(\hat{\mathcal{H}}_S - \mu_S\hat{N}_S)}$ from now on.

Taking into account that $t_i = -\infty$, we are therefore led to the following expression for the CGF of the hyperaccurate observable

$$\begin{aligned}\mathcal{G}_t(\eta) &= \ln \mathrm{Tr}[\hat{U}^\dagger(t, -\infty)e^{i\eta\hat{O}_h}\hat{U}(t, -\infty)e^{i\eta\hat{O}_h}\hat{\rho}(-\infty)] \\ &= \ln \mathrm{Tr}[\hat{U}^\dagger(t, -\infty)e^{i\eta\sum_l h(\epsilon_l)\hat{c}_l^\dagger\hat{c}_l}\hat{U}(t, -\infty) \\ &\quad \times e^{i\eta\sum_l h(\epsilon_l)\hat{c}_l^\dagger\hat{c}_l}\hat{\rho}(-\infty)].\end{aligned} \tag{B3}$$

Finally, a useful reformulation of the above result was found by Klich [37], which allowed to express the CGF as a determinant of second-quantization operators restricted to their single-particle subspace. The latter can be summarized as follows: let $\hat{X} = \sum_{ij} X_{ij}\hat{c}_i^\dagger\hat{c}_j$ be a fermionic bilinear operator and $\mathbf{X}$ denote the matrix with entries X_{ij}; then the following identity can be proven

$$\mathrm{Tr}[e^{\hat{X}}] = \det[1 + e^{\mathbf{X}}]. \tag{B4}$$

The same holds true for any product of fermionic bilinear operators, i.e., $\mathrm{Tr}[e^{\hat{X}}e^{\hat{Y}}] = \det[1 + e^{\mathbf{X}}e^{\mathbf{Y}}]$. For the problem at hand, one has that

$$\mathbf{O}_h = \mathrm{diag}(h(\epsilon_l)) \oplus \mathbf{1}_{SR} \tag{B5}$$

and

$$\boldsymbol{\rho}(-\infty) = \bigoplus_{\alpha=L,R,S} \mathrm{diag}(n_\alpha(\epsilon_\alpha)), \tag{B6}$$

where $n_\alpha(\epsilon_\alpha) = [1 + e^{-\beta_\alpha(\epsilon_\alpha-\mu_\alpha)}]^{-1}$. The application of Eq. (B4) to Eq. (B3) then leads to

$$\mathcal{G}_t(\eta) = \det[\mathbf{1}_{LSR} - \boldsymbol{\rho}(-\infty) + \boldsymbol{\rho}(-\infty)(\mathbf{U}^\dagger(t,-\infty) \times e^{i\eta\,\mathbf{O}_h}\mathbf{U}(t,-\infty)e^{i\eta\,\mathbf{O}_h})]. \tag{B7}$$

Equation (B7) represents the general expression for the current statistics of thermoelectric devices consisting of noninteracting fermions at any given time, and without any approximation. In the following section, we will consider the case of time-independent elastic scattering, also known as the Landauer-Büttiker regime, where the CGF reduces to the so-called Levitov-Lesovik expression.

APPENDIX C: ELASTIC SCATTERING

From now on, let us assume that the scattering region is of similar size or smaller compared to the relaxation lengthscales of the electrons (coherent scattering). Furthermore, we will focus our attention to elastic scattering, which implies that each electron moves from one reservoir to the other as a plane wave with energy ϵ. This condition is equivalent to requiring energy conservation and the validity of a large deviation principle, which is an assumption usually satisfied at the steady-state regime, whenever the size of the central system is negligible compared to the size of the baths (for which a thermodynamic limit is performed) [26]. In this case, electrons with different energies thus contribute to particle, energy, or any other such observable's (e.g., the hypercurrent's) statistics independently and thus $\mathcal{G}_t(\eta) = \int d\epsilon\, \mathcal{G}_t(\eta,\epsilon)$. Furthermore, one can describe the above problem by taking the long-time limit $t \to +\infty$ in Eq. (B3), and introducing the so-called *scattering matrix* $\hat{S} = \lim_{t\to\infty} e^{i(\hat{\mathcal{H}}_L+\hat{\mathcal{H}}_R)t}\hat{U}(t,-t)e^{-i(\hat{\mathcal{H}}_L+\hat{\mathcal{H}}_R)t}$. Exploiting the above considerations, the CGF Eq. (B7) then reduces to

$$\chi(\eta) := \lim_{t\to\infty}\frac{1}{t}\mathcal{G}_t(\eta) = \int d\epsilon\ \ln\det[\mathbf{1}_2 - \mathbf{n}_F(\epsilon) + \mathbf{n}_F(\epsilon)(\mathbf{S}^\dagger(\epsilon)\mathbf{X}(\epsilon)\mathbf{S}(\epsilon))\mathbf{X}^\dagger(\epsilon)], \tag{C1}$$

where $\mathbf{1}_2 = \begin{pmatrix}1 & 0\\ 0 & 1\end{pmatrix}$, and finally where we have introduced the two matrices

$$\mathbf{n}_F(\epsilon) = \begin{pmatrix}[1+e^{\beta_L(\epsilon-\mu_L)}]^{-1} & 0\\ 0 & [1+e^{\beta_R(\epsilon-\mu_R)}]^{-1}\end{pmatrix},$$
$$\mathbf{X}(\epsilon) \equiv \begin{pmatrix}e^{-i\eta h(\epsilon)} & 0\\ 0 & 1\end{pmatrix}. \tag{C2}$$

Upon expressing the scattering matrix in terms of reflection and transmission coefficients of the left and right leads $\mathbf{S}(\epsilon) = \begin{pmatrix}\mathrm{r}_{LL}(\epsilon) & \mathrm{t}_{LR}(\epsilon)\\ \mathrm{t}_{RL}(\epsilon) & \mathrm{r}_{RR}(\epsilon)\end{pmatrix}$, and making use of the following relations: (i) $\det[\mathbf{S}] = 1$, (ii) $|\mathrm{r}_{LL}(\epsilon)|^2 + |\mathrm{t}_{LR}(\epsilon)|^2 = 1$, (iii) $|\mathrm{r}_{RR}(\epsilon)|^2 + |\mathrm{t}_{RL}(\epsilon)|^2 = 1$, and (iv) $|\mathrm{t}_{LR}(\epsilon)|^2 = |\mathrm{t}_{RL}(\epsilon)|^2 \equiv \mathcal{T}(\epsilon)$, allows to finally arrive at the Levitov-Lesovik expression for the desired current

$$\chi(\eta) = \int d\epsilon\ \ln\{1 + \mathcal{T}(\epsilon)[(e^{h(\epsilon)\eta} - 1)n_L(\epsilon)(1-n_R(\epsilon)) + (e^{-h(\epsilon)\eta} - 1)n_R(\epsilon)(1-n_L(\epsilon))]\}. \tag{C3}$$

From this, Eqs. (4) and (5) of the main text follow directly by taking the appropriate derivatives. This calculation therefore allows us to conclude that, indeed, it is in principle possible to measure generic currents, given by some function $h(\epsilon)$. The caveat to do so is to measure an operator of the form (B2), interpreted in terms of the spectral theorem.

APPENDIX D: PERTURBATIVE FOURTH ORDER EXPANSION

In this section we will provide the detailed calculations of all the various currents, their fluctuations and the hyperaccurate bounds upon a fourth order Taylor expansion in the biases δ_β and $\delta_{\beta\mu}$, where

$$\beta_{L(R)} = \beta \pm \delta_\beta/2, \quad \beta_{L(R)}\mu_{L(R)} = \beta\mu \pm \delta_{\beta\mu}/2. \tag{D1}$$

Let us start by giving the perturbative expansions of the basic quantities appearing as integrands of Eqs. (4) and (5). First of all, let us define the variable $x \equiv \beta(\epsilon-\mu)$. This means that we will do the expansions of the following quantities of interest in $\delta_x = \delta_\beta\epsilon - \delta_{\beta\mu}$. Moreover, for easiness of notation, let us define $f_n \equiv f^{(n)}(x)$, with $f = (e^{\beta(\epsilon-\mu)}+1)^{-1}$ being the Fermi function evaluated at the average temperature and chemical potential.

(i) $\Delta f = f_1\delta_x + \frac{f_3}{24}\delta_x^3 + O(\delta_x^5)$;
(ii) $g = -2f_1 - \frac{f_3}{4}\delta_x^2 - \frac{f_5}{192}\delta_x^4 + O(\delta_x^5)$;
(iii) $\Delta f^2 = f_1^2\delta_x^2 + \frac{f_1 f_3}{12}\delta_x^4 + O(\delta_x^5)$.

Inserting these expansions back into the expressions for the average currents and variances allows to obtain the desired results. In particular, let us define the quantity

$$\phi_m^n = -\int \epsilon^n f_m \mathcal{T}. \tag{D2}$$

Notice that in the main text, in particular in Eq. (15), we adopted the simplified notation

$$\theta_n \equiv \phi_1^n = -\int \epsilon^n f_1\mathcal{T} = \int d\epsilon\epsilon^n f(1-f)\mathcal{T}, \tag{D3}$$

where the identity $f_1 = -f(1-f)$ has been used.

By using Eq. (D2), after some simple algebra, one obtains the following expressions for the average currents.

(i) The average particle current:

$$J_N = -\delta_\beta\phi_1^1 + \delta_{\beta\mu}\phi_1^0 + \frac{1}{24}\sum_{k=0}^{3}\binom{3}{k}(-1)^k\delta_\beta^k\delta_{\beta\mu}^{3-k}\,\phi_3^k + O(\delta_\beta^5,\delta_{\beta\mu}^5). \tag{D4}$$

(ii) The average energy current:

$$J_E = -\delta_\beta \phi_1^2 + \delta_{\beta\mu}\phi_1^1 + \frac{1}{24}\sum_{k=0}^{3}\binom{3}{k}(-1)^k \delta_\beta^k \delta_{\beta\mu}^{3-k}\,\phi_3^{k+1} + O\big(\delta_\beta^5, \delta_{\beta\mu}^5\big). \tag{D5}$$

(iii) The entropy production:

$$\sigma = \delta_\beta^2\phi_1^2 - 2\delta_\beta\delta_{\beta\mu}\phi_1^1 + \delta_{\beta\mu}^2\phi_1^0 + \frac{1}{24}\left[\sum_{k=0}^{4}\binom{4}{k}(-1)^k \delta_\beta^k \delta_{\beta\mu}^{4-k}\,\phi_3^k\right] + O\big(\delta_\beta^5, \delta_{\beta\mu}^5\big)$$
$$\equiv \sigma^{(2)} + \Theta_4/24 + O\big(\delta_\beta^5, \delta_{\beta\mu}^5\big), \tag{D6}$$

where $\sigma^{(2)} \equiv \delta_\beta^2\theta_2 - 2\delta_\beta\delta_{\beta\mu}\theta_1 + \delta_{\beta\mu}^2\theta_0$ and $\Theta_4 \equiv \int d\epsilon(\delta_{\beta\mu} - \epsilon\delta_\beta)^4 f(1-f)(1-6f+6f^2)\mathcal{T}$. This is the result reported in Eq. (14) of the main text.

(iv) The particle variance:

In order to express the variances and the hyperaccurate bounds in a similar compact fashion, we introduce the last quantity given by

$$\psi_{lm}^n = \int d\epsilon\ \epsilon^n f_l f_m \mathcal{T}(1-\mathcal{T}). \tag{D7}$$

By making use of it, one finds the following expressions

(1) The particle variance

$$\Delta_N^2 = 2\phi_1^0 + \left[\sum_{k=0}^{2}\binom{2}{k}(-1)^k\delta_\beta^k\delta_{\beta\mu}^{2-k}\left(\psi_{11}^k + \frac{\phi_3^k}{4}\right)\right] + \left[\sum_{k=0}^{4}\binom{4}{k}(-1)^k\delta_\beta^k\delta_{\beta\mu}^{4-k}\left(\frac{\psi_{13}^k}{12} + \frac{\phi_5^k}{192}\right)\right] + O\big(\delta_\beta^5, \delta_{\beta\mu}^5\big). \tag{D8}$$

(2) The energy variance:

$$\Delta_E^2 = 2\phi_1^2 + \left[\sum_{k=0}^{2}\binom{2}{k}(-1)^k\delta_\beta^k\delta_{\beta\mu}^{2-k}\left(\psi_{11}^{k+2} + \frac{\phi_3^{k+2}}{4}\right)\right] + \left[\sum_{k=0}^{4}\binom{4}{k}(-1)^k\delta_\beta^k\delta_{\beta\mu}^{4-k}\left(\frac{\psi_{13}^{k+2}}{12} + \frac{\phi_5^{k+2}}{192}\right)\right] + O\big(\delta_\beta^5, \delta_{\beta\mu}^5\big). \tag{D9}$$

(3) The energy-particle correlation function:

$$C = 2\phi_1^1 + \left[\sum_{k=0}^{2}\binom{2}{k}(-1)^k\delta_\beta^k\delta_{\beta\mu}^{2-k}\left(\psi_{11}^{k+1} + \frac{\phi_3^{k+1}}{4}\right)\right] + \left[\sum_{k=0}^{4}\binom{4}{k}(-1)^k\delta_\beta^k\delta_{\beta\mu}^{4-k}\left(\frac{\psi_{13}^{k+1}}{12} + \frac{\phi_5^{k+1}}{192}\right)\right] + O\big(\delta_\beta^5, \delta_{\beta\mu}^5\big). \tag{D10}$$

It is important to stress that all the terms in the above (and below) expressions proportional to the various ψs vanish in the case of a box-car transmission function. Finally, the two hyperaccurate bounds $\mathcal{S}_{\text{hyp}}$ [Eq. (9)] and $\mathcal{S}_{\text{thyp}}$ [Eq. (11)] are given by

$$\mathcal{S}_{\text{hyp}} = \mathcal{S}_{\text{thyp}} = \int \frac{\mathcal{T}\Delta f^2}{g + [1-\mathcal{T}]\Delta f^2} = \int \left[-\frac{\mathcal{T}f_1}{2}\delta_x^2 + \left(\frac{\mathcal{T}f_3}{48} - \frac{\mathcal{T}(1-\mathcal{T})f_1^2}{4}\right)\delta_x^4\right] + O\big(\delta_\beta^5, \delta_{\beta\mu}^5\big), \tag{D11}$$

$$= \frac{\delta_\beta^2\phi_1^2 - 2\delta_\beta\delta_{\beta\mu}\phi_1^1 + \delta_{\beta\mu}^2\phi_1^0}{2} - \frac{1}{48}\left[\sum_{k=0}^{4}\binom{4}{k}(-1)^k\delta_\beta^k\delta_{\beta\mu}^{4-k}\left(\phi_3^k + 12\psi_{11}^k\right)\right] + O\big(\delta_\beta^5, \delta_{\beta\mu}^5\big). \tag{D12}$$

The last term can also be rearranged more clearly into the two contributions $\Theta_4 + 6\Psi_4$ introduced in Eq. (16).

[1] A. C. Barato and U. Seifert, Thermodynamic Uncertainty Relation for Biomolecular Processes, Phys. Rev. Lett. **114**, 158101 (2015).

[2] T. R. Gingrich, J. M. Horowitz, N. Perunov, and J. L. England, Dissipation Bounds All Steady-State Current Fluctuations, Phys. Rev. Lett. **116**, 120601 (2016).

[3] P. Pietzonka, A. C. Barato, and U. Seifert, Universal bounds on current fluctuations, Phys. Rev. E **93**, 052145 (2016).

[4] J. M. Horowitz and T. R. Gingrich, Thermodynamic uncertainty relations constrain nonequilibrium fluctuations, Nat. Phys. **16**, 15 (2019).

[5] M. Polettini, A. Lazarescu, and M. Esposito, Tightening the uncertainty principle for stochastic currents, Phys. Rev. E **94**, 052104 (2016).

[6] T. R. Gingrich, G. M. Rotskoff, and J. M. Horowitz, Inferring dissipation from current fluctuations, J. Phys. A: Math. Theor. **50**, 184004 (2017).

[7] P. Pietzonka and U. Seifert, Universal Trade-Off between Power, Efficiency, and Constancy in Steady-State Heat Engines, Phys. Rev. Lett. **120**, 190602 (2018).

[8] T. Van Vu and Y. Hasegawa, Thermodynamic uncertainty relations under arbitrary control protocols, Phys. Rev. Res. **2**, 013060 (2020).

[9] G. Paneru, S. Dutta, T. Tlusty, and H. K. Pak, Reaching and violating thermodynamic uncertainty bounds in information engines, Phys. Rev. E **102**, 032126 (2020).

[10] D. M. Busiello and S. Pigolotti, Hyperaccurate currents in stochastic thermodynamics, Phys. Rev. E **100**, 060102 (2019).

[11] Y. Hasegawa and T. Van Vu, Uncertainty relations in stochastic processes: An information inequality approach, Phys. Rev. E **99**, 062126 (2019).

[12] B. K. Agarwalla and D. Segal, Assessing the validity of the thermodynamic uncertainty relation in quantum systems, Phys. Rev. B **98**, 155438 (2018).

[13] K. Ptaszyński, Coherence-enhanced constancy of a quantum thermoelectric generator, Phys. Rev. B **98**, 085425 (2018).

[14] S. Saryal, H. Friedman, D. Segal, and B. K. Agarwalla, Thermodynamic uncertainty relation in thermal transport, Phys. Rev. E **100**, 042101 (2019).

[15] G. Guarnieri, G. T Landi, S. R. Clark, and J. Goold, Thermodynamics of precision in quantum non equilibrium steady states, Phys. Rev. Res. **1**, 033021 (2019).

[16] J. Liu and D. Segal, Thermodynamic uncertainty relation in quantum thermoelectric junctions, Phys. Rev. E **99**, 062141 (2019).

[17] L. M. Cangemi, M. Carrega, A. De Candia, V. Cataudella, G. De Filippis, M. Sassetti, and G. Benenti, Optimal energy conversion through antiadiabatic driving breaking time-reversal symmetry, Phys. Rev. Res. **3**, 013237 (2021).

[18] T. Ehrlich and G. Schaller, Broadband frequency filters with quantum dot chains, Phys. Rev. B **104**, 045424 (2021).

[19] A. A. S. Kalaee, A. Wacker, and P. P. Potts, Violating the thermodynamic uncertainty relation in the three-level maser, Phys. Rev. E **104**, L012103 (2021).

[20] S. Saryal, O. Sadekar, and B. K. Agarwalla, Thermodynamic uncertainty relation for energy transport in a transient regime: A model study, Phys. Rev. E **103**, 022141 (2021).

[21] J. Liu and D. Segal, Coherences and the thermodynamic uncertainty relation: Insights from quantum absorption refrigerators, Phys. Rev. E **103**, 032138 (2021).

[22] A. M. Timpanaro, G. Guarnieri, and G. T. Landi, The most precise quantum thermoelectric, arXiv:2106.10205.

[23] S. Datta, *Electronic Transport in Mesoscopic Systems* (Cambridge University Press, Cambridge, UK, 1997).

[24] For large biases, charge accumulation in the leads can become an issue [38,39]. Here we assume this can be avoided.

[25] L. Levitov and G. Lesovik, Charge distribution in quantum shot noise, Pis'ma Zh. Eksp. Teor. Fiz. **58**, 225 (1993) [JETP Lett. **58**, 230 (1993)].

[26] M. Esposito, U. Harbola, and S. Mukamel, Nonequilibrium fluctuations, fluctuation theorems, and counting statistics in quantum systems, Rev. Mod. Phys. **81**, 1665 (2009).

[27] M. Büttiker, Scattering theory of current and intensity noise correlations in conductors and wave guides, Phys. Rev. B **46**, 12485 (1992).

[28] G. D. Mahan and J. O. Sofo, The best thermoelectric, Proc. Natl. Acad. Sci. USA **93**, 7436 (1996).

[29] R. S. Whitney, Most Efficient Quantum Thermoelectric at Finite Power Output, Phys. Rev. Lett. **112**, 130601 (2014).

[30] M. Gerry and D. Segal, Absence and recovery of cost-precision tradeoff relations in quantum transport, Phys. Rev. B **105**, 155401 (2022).

[31] M. Büttiker, Quantized transmission of a saddle-point constriction, Phys. Rev. B **41**, 7906 (1990).

[32] J. Settino, R. Citro, F. Romeo, V. Cataudella, and C. A. Perroni, Ballistic transport through quantum point contacts of multiorbital oxides, Phys. Rev. B **103**, 235120 (2021).

[33] Gauge invariance means that a shift $\mu_i \to \mu_i + \eta$ in both chemical potentials is followed by a shift $h(\epsilon) \to h(\epsilon - \eta)$.

[34] G. Benenti, G. Casati, K. Saito, and R. S. Whitney, Fundamental aspects of steady-state conversion of heat to work at the nanoscale, Phys. Rep. **694**, 1 (2017).

[35] J. Ehrich, Tightest bound on hidden entropy production from partially observed dynamics, J. Stat. Mech.: Theory Exp. (2021) 083214.

[36] K. Fujii, Introduction to the Rotating Wave Approximation (RWA): Two coherent oscillations, J. Modern Phys. **8**, 2042 (2017).

[37] I. Klich, An elementary derivation of Levitov's formula, in *Quantum Noise in Mesoscopic Physics*, edited by Y. V. Nazarov, NATO Science Series, Vol. 97 (Springer, Dordrecht, Netherlands, 2003), pp. 397–402.

[38] D. Sánchez and R. López, Scattering Theory of Nonlinear Thermoelectric Transport, Phys. Rev. Lett. **110**, 026804 (2013).

[39] T. Christen and M. Büttiker, Gauge-invariant nonlinear electric transport in mesoscopic conductors, Europhys. Lett. **35**, 523 (1996).